

# Effect of celastrol on toll-like receptor 4-mediated inflammatory response in free fatty acid-induced HepG2 cells

LI-PING HAN, BEI SUN, CHUN-JUN LI, YUN XIE and LI-MING CHEN

Key Laboratory of Hormones and Development (Ministry of Health), Tianjin Key Laboratory of Metabolic Diseases, Tianjin Metabolic Diseases Hospital and Tianjin Institute of Endocrinology, Tianjin Medical University, Tianjin 300070, P.R. China

Received February 13, 2018; Accepted July 10, 2018

DOI: 10.3892/ijmm.2018.3775

**Abstract.** Toll-like receptor 4 (TLR4)-mediated immune and inflammatory signaling serves a pivotal role in the pathogenesis of nonalcoholic fatty liver disease (NAFLD). Our previous study demonstrated that celastrol treatment was able to improve hepatic steatosis and inhibit the TLR4 signaling cascade pathway in type 2 diabetic rats. The present study aimed to investigate the effects of celastrol on triglyceride accumulation and inflammation in steatotic HepG2 cells, and the possible mechanisms responsible for the regulation of cellular responses following TLR4 gene knockdown by small interfering RNA (siRNA) *in vitro*. A cell model of hepatic steatosis was prepared by exposing the HepG2 cells to free fatty acid (FFA) in the absence or presence of celastrol. Intracellular triglycerides were visualized by Oil red O staining, and the TLR4/myeloid differentiation primary response 88 (MyD88)/nuclear factor- $\kappa$ B (NF- $\kappa$ B) signaling cascade pathway were investigated. To directly elucidate whether TLR4 was the blocking target of celastrol upon FFA exposure, the cellular response to inflammation was determined upon transfection with TLR4 siRNA. The results revealed that celastrol significantly reduced triglyceride accumulation in the steatotic HepG2 cells, and downregulated the expression levels of TLR4, MyD88 and phospho-NF- $\kappa$ Bp65, as well as of the downstream inflammatory cytokines interleukin-1 $\beta$  and tumor necrosis factor  $\alpha$ . Knockdown of TLR4 also alleviated FFA-induced inflammatory response. In addition, co-treatment with TLR4 siRNA and celastrol further attenuated the expression of inflammatory mediators. These results suggest that celastrol exerts its protective effect partly via inhibiting

the TLR4-mediated immune and inflammatory response in steatotic HepG2 cells.

## Introduction

The hallmarks of nonalcoholic steatohepatitis (NASH), which is the progressive form of nonalcoholic fatty liver disease (NAFLD), are inflammation and hepatocyte injury, and this disease is currently a growing public health issue. In NASH/NAFLD, innate immune activation serves a key role in triggering and amplifying hepatic inflammation (1,2). Fatty acid accumulation, in particular saturated fatty acids, in the liver have been reported to activate a series of pro-inflammatory signaling pathways, leading to the activation of both the innate and adaptive types of immune response (3,4). Previous studies revealed that toll-like receptors (TLRs), the sensors of endogenous and microbial danger signals, are expressed and activated in parenchymal and innate immune cells in the liver, consequently contributing to NASH (5,6).

TLR4 is a well-known pattern recognition receptor that serves a fundamental regulatory role in promoting the progression of chronic liver diseases (7). Hepatic tissue injured by toxic lipid molecules (lipotoxicity) serves an essential role in the recruitment of innate immunity involving TLR4 (8). Additionally, the TLR4 signaling pathway initiated through the downstream signaling ligand activates nuclear factor- $\kappa$ B (NF- $\kappa$ B) and induces the expression of inflammatory response-associated genes. These changes promote signaling cascades leading to injury amplification (9). Thus, the relevance of modulating these inflammatory signaling pathways as potential novel therapeutic strategies for NASH urgently requires further investigation.

As a potent immunosuppressive and anti-inflammatory agent, celastrol (C<sub>29</sub>H<sub>38</sub>O<sub>4</sub>) has been widely used for the treatment of various autoimmune diseases (10,11). The latest research on celastrol has mainly focused on ameliorating metabolic disease and relevant organ injury. Liu *et al* (12) reported that celastrol is a leptin sensitizer and a promising agent for the pharmacological treatment of obesity. Furthermore, it has been demonstrated that celastrol alleviated high-fat diet-mediated cardiovascular injury via mitigating oxidative stress and improving lipid metabolism (13). The study by Kim *et al* (14) also reported that administration of celastrol resulted in significant decreases in adiposity in multiple

---

*Correspondence to:* Dr Li-Ming Chen, Key Laboratory of Hormones and Development (Ministry of Health), Tianjin Key Laboratory of Metabolic Diseases, Tianjin Metabolic Diseases Hospital and Tianjin Institute of Endocrinology, Tianjin Medical University, 66 Tongan Road, Heping, Tianjin 300070, P.R. China  
E-mail: xfx22081@vip.163.com

**Key words:** celastrol, HepG2, toll-like receptor 4, inflammation, RNA interference

organs in diabetic db/db mice. In addition, this administration improved renal functional and structural changes through the metabolic and NF- $\kappa$ B-inhibitory activity, and the cytokine-suppressing activities in the kidney (14). Our previous study firstly confirmed that celastrol provided a protective effect against fatty hepatic injury in type 2 diabetic rats through suppression of the inflammatory process (15). However, our research only performed preliminary observational experiments *in vivo*, while the definite mechanisms of celastrol remain to be studied *in vitro*.

Numerous studies (5-8) have reported that activation of the TLR4-mediated inflammatory pathway in hepatocytes serves an important role in the early stages of NAFLD. Therefore, it can be hypothesized that celastrol may protect hepatocytes against lipid deposition and inflammatory response via inhibiting TLR4 activation, and subsequently suppressing signaling cascades and avoiding the release of inflammatory response factors. Thus, in the present study, small interfering RNA (siRNA) transfection was performed to evaluate the significance of TLR4 and the contribution of the TLR4-mediated intracellular signaling pathway to the inflammation in free fatty acid (FFA)-induced HepG2 cells. Furthermore, the effects of celastrol in these cells and the associated mechanisms were investigated.

## Materials and methods

**Cell culture.** HepG2 cells were supplied by the Department of Immunology of Tianjin Medical University (Tianjin, China). Although HepG2 cells originate from hepatoblastoma (16), the study by Gómez-Lechón *et al* (17) demonstrated that fat overaccumulation is induced in hepatic cells by FFA, and that human hepatocytes and HepG2 cells behave nearly the same. HepG2 cells are, therefore, generally accepted as a promising alternative to human hepatocytes for use as a cellular model of steatosis (17-19). HepG2 cells were cultured in Dulbecco's modified Eagle's medium (DMEM; Gibco; Thermo Fisher Scientific, Inc., Waltham, MA, USA) supplemented with 10% fetal bovine serum (FBS; Gibco; Thermo Fisher Scientific, Inc.) and 1% penicillin/streptomycin at 37°C and 5% CO<sub>2</sub>. Purified celastrol was purchased from Merck KGaA (Calbiochem; Darmstadt, Germany) and stored at -20°C. Celastrol was freshly dissolved in 10% dimethyl sulfoxide prior to use. Palmitate acid and oleic acid were purchased from Sigma-Aldrich (Merck KGaA) and dissolved in isopropyl alcohol. When 70-80% confluency was reached, the HepG2 cells were cultured in serum-free DMEM with 0.5% bovine serum albumin (BSA; Sigma-Aldrich; Merck KGaA) or different concentrations of FFA (palmitate acid: Oleic acid ratio, 1:2) (17) or different concentrations of celastrol, as specified below.

**Cell viability assay.** Cell viability was assessed using the Cell Counting Kit-8 (CCK8) assay (Jiancheng Bioengineering Institute, Nanjing, China). Briefly, HepG2 cells were seeded in a 96-well plate at a density of  $1 \times 10^4$  cells/well. Following treatment with various concentrations of FFA (0.25, 0.5, 1.0 and 2.0 mM) or celastrol (0.1, 0.2, 0.5, 1.0, 1.5 and 2.0  $\mu$ M) in triplicate for 20 h, 10  $\mu$ l CCK8 was added to each well and incubated for an additional 4 h at 37°C in an atmosphere

containing 5% CO<sub>2</sub>. The absorbance at 450 nm was then measured using a microplate reader (Thermo Fisher Scientific, Inc.). The inhibition of cytotoxicity was calculated as a fraction of the control and is expressed as the percentage of cell viability.

**Oil red O staining.** Accumulation of triglycerides in the treated HepG2 cells was visualized by Oil red O staining (Sigma-Aldrich; Merck KGaA). Briefly, cells were seeded in a 6-well plate at a density of  $3 \times 10^5$  cells/well and then stained with freshly diluted Oil red O solution for 30 min at room temperature. The sections were then washed with PBS twice, and the nuclei of the cells were counterstained with hematoxylin for 1 min. To examine lipid accumulation, cell images were captured with a microscope (Olympus Corporation, Tokyo, Japan).

**Intracellular triglyceride test.** HepG2 cells were seeded at a density of  $3 \times 10^5$  cells/well in a 6-well plate. Intracellular triglyceride accumulation was determined following lipid extraction as described previously by Schwartz and Wolins (20), followed by spectrophotometry determination using a triglyceride assay kit (cat no. A110-2; Nanjing Jiancheng Bioengineering Institute, Nanjing, China) according to the manufacturer's protocol. Subsequently, the absorbance at 510 nm was measured using a microplate reader (Thermo Fisher Scientific, Inc.). The protein concentration was determined using a BCA protein assay kit (Thermo Fisher Scientific, Inc.). Values of triglyceride were normalized to the total protein concentration. Intracellular triglyceride content (mmol/g protein)=intracellular triglyceride concentration (mmol/l)/protein concentration (g/l).

**Knockdown of TLR4 by siRNA.** HepG2 cells were transiently transfected with fluorescein amidite (FAM)-labeled siRNA that targeted TLR4 or with negative control siRNA obtained from GenePharma Co., Ltd. (Shanghai, China), using Lipofectamine® 2000 (Invitrogen; Thermo Fisher Scientific, Inc.). Three human TLR4 siRNA constructs were examined, and their sequences are shown in Table I. Briefly, 10  $\mu$ l of 20  $\mu$ M siRNA and 5  $\mu$ l Lipofectamine® 2000 were suspended in 250  $\mu$ l of serum-free Opti-MEM medium (Gibco; Thermo Fisher Scientific, Inc.), forming an siRNA/Lipofectamine mixture. The mixture was then added to  $2 \times 10^5$  HepG2 cells cultured in a 6-well plate. Following 24 h of transfection, the transfection efficiency was observed using fluorescence microscopy (Olympus Corporation). The knockdown effects of TLR4 were confirmed using reverse transcription-quantitative polymerase chain reaction (RT-qPCR) and western blotting. Following transfection, the medium was changed to regular medium and the cells were treated with BSA, FFAs and celastrol combinations for 24 h, as described. HepG2 cells were divided into seven groups, including the normal control (NC), and groups treated with 0.5 mM FFA, negative siRNA + 0.5 mM FFA, TLR4 siRNA + 0.5 mM FFA, 0.5 mM FFA + 0.5  $\mu$ M celastrol, negative siRNA + 0.5 mM FFA + 0.5  $\mu$ M celastrol, and TLR4 siRNA + 0.5 mM FFA + 0.5  $\mu$ M celastrol.

**RT-qPCR analysis.** Total RNA was isolated from HepG2 cells with TRIzol reagent (Invitrogen; Thermo Fisher Scientific, Inc.). The concentration of total RNA was determined by spec-

Table I. Sequences of TLR4 siRNA and negative control siRNA.

siRNA	Sequence
TLR4 siRNA1	Forward: 5'-CCUGGUGAGUGUGACUAUUTT-3' Reverse: 5'-AAUAGUCACACUCACCAGGTT-3'
TLR4 siRNA2	Forward: 5'-CCUGAACCUAUGAACUUUTT-3' Reverse: 5'-AAAGUUCAUAGGGUUCAGGTT-3'
TLR4 siRNA3	Forward: 5'-GGAUUUAUCCAGGUGUGAATT-3' Reverse: 5'-UUCACACCUGGAUAAAUCCTT-3'
Negative control siRNA	Forward: 5'-UUCUCCGAACGUGUCACGUTT-3' Reverse: 5'-ACGUGACACGUUCGGAGAATT-3'

TLR4, toll-like receptor 4; siRNA, small interfering RNA.

trophotometry (TECAN Infinite F200PRO microplate reader; Tecan Group, Ltd., Mannedorf, Switzerland). Next, cDNA synthesis was performed using the High-Capacity cDNA Reverse Transcription kit (Applied Biosystems; Thermo Fisher Scientific, Inc.) according to the manufacturer's protocol. qPCR was performed in a total volume of 10  $\mu$ l, containing 5  $\mu$ l 2X SYBR Green Premix Ex Taq<sup>TM</sup> (Takara Bio, Inc., Otsu, Japan), 1  $\mu$ l cDNA, 3  $\mu$ l distilled water and 0.5  $\mu$ l of each primer. qPCR was conducted in a thermal cycler (Bio-Rad Laboratories, Inc., Hercules, CA, USA), with initial denaturation performed at 95°C for 3 min, followed by 45 cycles of denaturation for 10 sec at 95°C, annealing for 30 sec at 60°C, and extension for 20 sec at 72°C. All primers used in qPCR were synthesized by Augct DNA-Syn Biotechnology Co., Ltd. (Beijing, China), and the human glyceraldehyde-3-phosphate dehydrogenase (GAPDH) gene served as the housekeeping gene. The following specific primers were used: Human TLR4 forward, 5'-GCAATGGATCAAGGACCAGA-3', and reverse, 5'-CTACAAGCACACTGAGGACC-3'; and human GAPDH forward, 5'-CTCCTCCACCTTTGACGCTG-3' and reverse, 5'-TCCTCTTGCTGCTCTTGCTGG-3'. The mRNA levels were normalized against the mRNA levels of the housekeeping gene GAPDH. Data were analyzed using the CFX Manager software (version 1.6; Bio-Rad Laboratories, Inc.). Relative quantification of the target gene mRNA was performed using the  $2^{-\Delta\Delta C_q}$  method and normalized to the internal control (21).

**Western blotting.** Proteins of HepG2 cell samples were extracted using a radioimmunoprecipitation assay buffer (Thermo Fisher Scientific, Inc.) on ice, according to the manufacturer's protocol, and the protein concentrations were then measured using a BCA protein assay kit (Thermo Fisher Scientific, Inc.). An equal amount of protein from each sample was subjected to 12% sodium dodecyl sulfate-polyacrylamide gel electrophoresis and then transferred to polyvinylidene difluoride membranes (EMD Millipore, Billerica, MA, USA). Membranes were blocked with 5% milk for 2 h at room temperature and subsequently incubated overnight at 4°C with primary antibodies against TLR4 (1:1,000; cat no. ab13867; Abcam, Cambridge, UK), myeloid differentiation primary response 88 (MyD88; 1:500; cat no. ab2064; Abcam), phospho-NF- $\kappa$ Bp65 (1:2,000; cat no. ab86299; Abcam), NF- $\kappa$ Bp65 (1:2,000; cat no. ab16502; Abcam), interleukin

(IL)-1 $\beta$  (1:1,000; cat no. ab2105; Abcam) and tumor necrosis factor  $\alpha$  (TNF $\alpha$ ; 1:1,000; cat no. ab8348; Abcam), as well as the internal control  $\beta$ -actin (1:10,000; cat no. KM9001T; Tianjin Sungene Biotech Co., Ltd., Tianjin, China). Next, membranes were washed twice for 10 min in 1X TBST and then incubated with horseradish peroxidase-conjugated goat anti-rabbit or goat anti-mouse secondary antibodies (all 1:5,000; Tianjin Sungene Biotech Co., Ltd.) at room temperature for 2 h. Membranes were then washed twice for 10 min in 1X TBST. Proteins were visualized by enhanced chemiluminescence (EMD Millipore), and blots were scanned in a dark room. Densitometry analysis of bands was performed with the ImageJ software (National Institutes of Health, Bethesda, MD, USA).

**Statistical analysis.** Statistical analysis was performed using SPSS version 17.0 (SPSS, Inc., Chicago, IL, USA) and GraphPad Prism version 5.0 software (GraphPad Software, Inc., La Jolla, CA, USA). Quantitative data are expressed as the mean  $\pm$  standard error of the mean. The statistical significance of the data obtained was evaluated using the one-way analysis of variance, followed by the least significant difference-test. A value of  $P < 0.05$  was considered to denote a statistically significant difference.

## Results

**Effects of celastrol on triglycerides accumulation in FFAs-induced HepG2 cells.** The chemical structure of celastrol is presented in Fig. 1A. The cytotoxic effects of various concentrations FFA (0.25, 0.5, 1.0 and 2.0 mM) and celastrol (0.1, 0.2, 0.5, 1.0, 1.5 and 2.0  $\mu$ M) in HepG2 cells were initially investigated. A CCK8 assay was used to quantify the effects on HepG2 cell growth. As illustrated in Fig. 1B, there were no significant difference in cell viability between the NC group and cells treated with 0.25 or 0.5 mM FFA. However, HepG2 cells treated with 1.0 and 2.0 mM FFA exhibited a significant decrease in cell viability by  $\sim 25.7$  and  $\sim 69.3\%$ , respectively (both  $P < 0.05$ ). Therefore, 0.5 mM FFA was used as the optimal concentration for the cell model of hepatic steatosis. Furthermore, as illustrated in Fig. 1C, there were no significant difference in cell viability between the NC, and the 0.1, 0.2 and 0.5  $\mu$ M celastrol-treated groups. However, HepG2 cells treated with 1.0, 1.5 and 2.0  $\mu$ M celastrol exhibited a significant

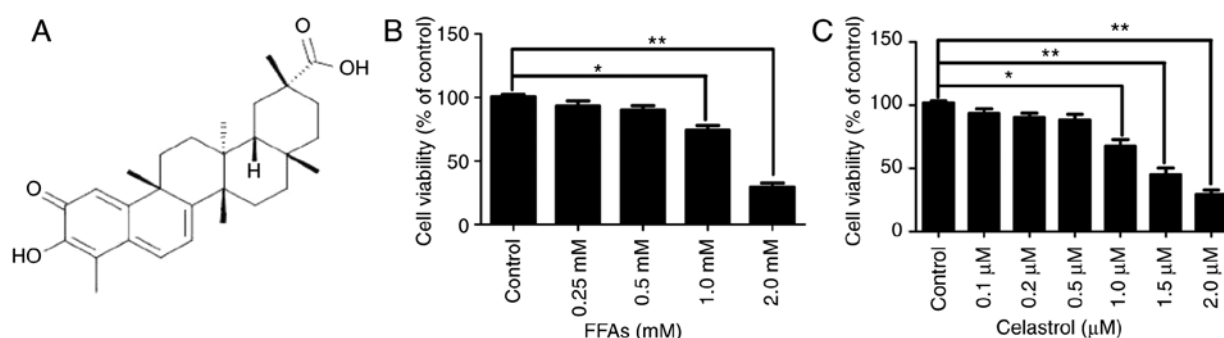


Figure 1. Cytotoxic effects of FFA and celastrol in HepG2 cells. (A) Chemical structure of celastrol. In order to determine the optimal concentration for subsequent experiments, the cytotoxic effects of FFA (0.25, 0.5, 1.0 and 2.0 mM) and celastrol (0.1, 0.2, 0.5, 1.0, 1.5 and 2.0 μM) in HepG2 cells were investigated. HepG2 cells were incubated with the indicated concentrations of (B) FFA and (C) celastrol for 24 h, and cell viability was measured by the Cell Counting Kit-8 assay. Data are expressed as the mean  $\pm$  standard error of the mean (n=6). \*P<0.05 and \*\*P<0.01. FFA, free fatty acid.

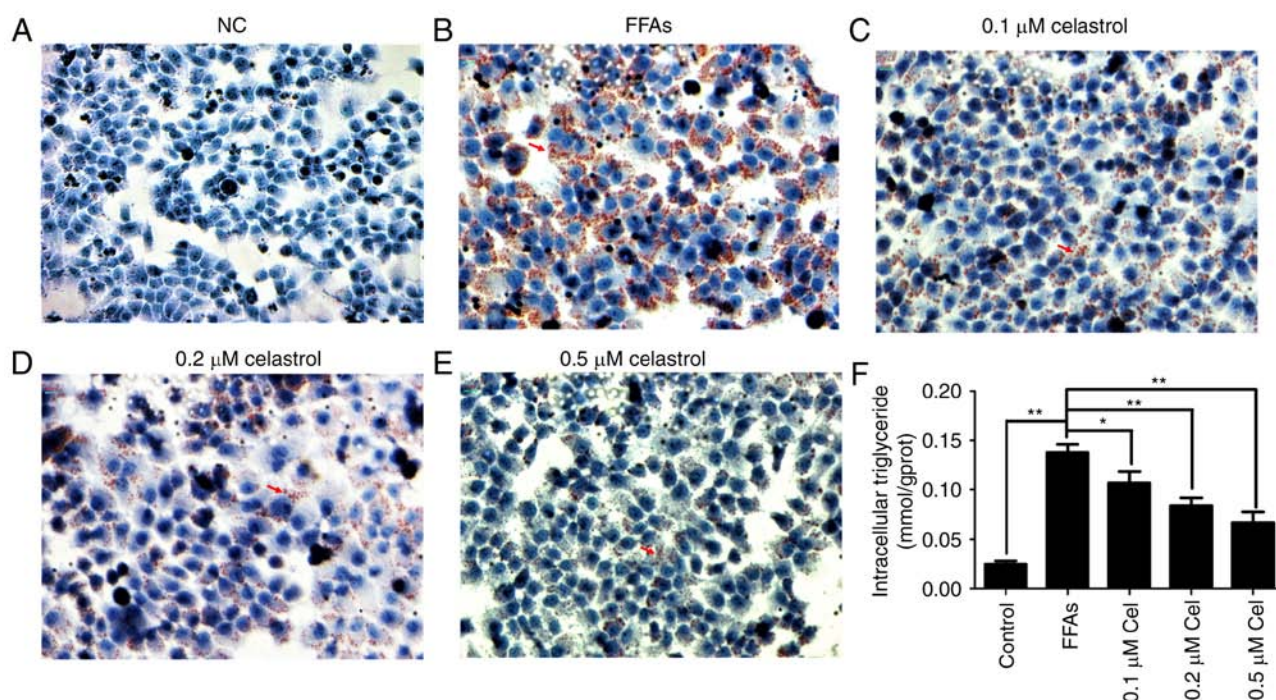


Figure 2. Effects of celastrol on triglyceride accumulation in the FFA-induced HepG2 cells. A cell model of hepatic steatosis was prepared by exposing HepG2 cells to 0.5 mM FFA and then incubating with 0.1, 0.2 and 0.5 μM celastrol for 24 h. Oil red O staining is shown in the (A) normal control, (B) 0.5 mM FFA, (C) 0.5 mM FFA + 0.1 μM celastrol, (D) 0.5 mM FFA + 0.2 μM celastrol and (E) 0.5 mM FFA + 0.5 μM celastrol groups (magnification, x400). Red arrows indicate lipid droplets. (F) Levels of intracellular triglycerides were analyzed by an enzymatic assay. Data are shown as the mean  $\pm$  standard error of the mean (n=6). \*P<0.05 and \*\*P<0.01. FFA, free fatty acid.

decrease in cell viability by approximately 22.3, 55 and 70.7%, respectively (all P<0.05).

Oil red O staining was then used to evaluate the effect of celastrol on lipid deposition. As shown in Fig. 2A-E, HepG2 cells in the 0.5 mM FFA-treated group presented widespread deposition of red lipid droplets as compared with the NC group. By contrast, the lipid droplets were significantly decreased in the FFA + celastrol (0.1, 0.2 and 0.5 μM) treatment groups, particularly in the 0.5 μM celastrol-treated group. As shown in Fig. 2F, the levels of intracellular triglycerides were significantly higher in 0.5 mM FFA-induced HepG2 cells compared with those of the NC group. In addition, intracellular triglyceride levels were decreased in the celastrol-treated group in a dose-dependent manner, with 0.5 μM celastrol exhibiting the highest efficacy. Therefore, based on the

data of the present study, 0.5 μM celastrol was selected as the optimal concentration for subsequent experiments.

*Effects of celastrol on the expression levels of TLR4 and downstream key inflammatory mediators in FFA-induced HepG2 cells.* To examine the anti-inflammatory effect of celastrol, HepG2 cells were treated with 0.5 μM celastrol, followed by stimulation with 0.5 mM FFA for 24 h. RT-qPCR and western blotting were subsequently used to quantify the effects of celastrol on TLR4 signaling in the FFA-induced HepG2 cells. As illustrated in Fig. 3A and B, FFAs significantly increased the expression levels of TLR4 mRNA and protein compared with those of the NC group. However, co-treatment with 0.5 μM celastrol greatly inhibited TLR4



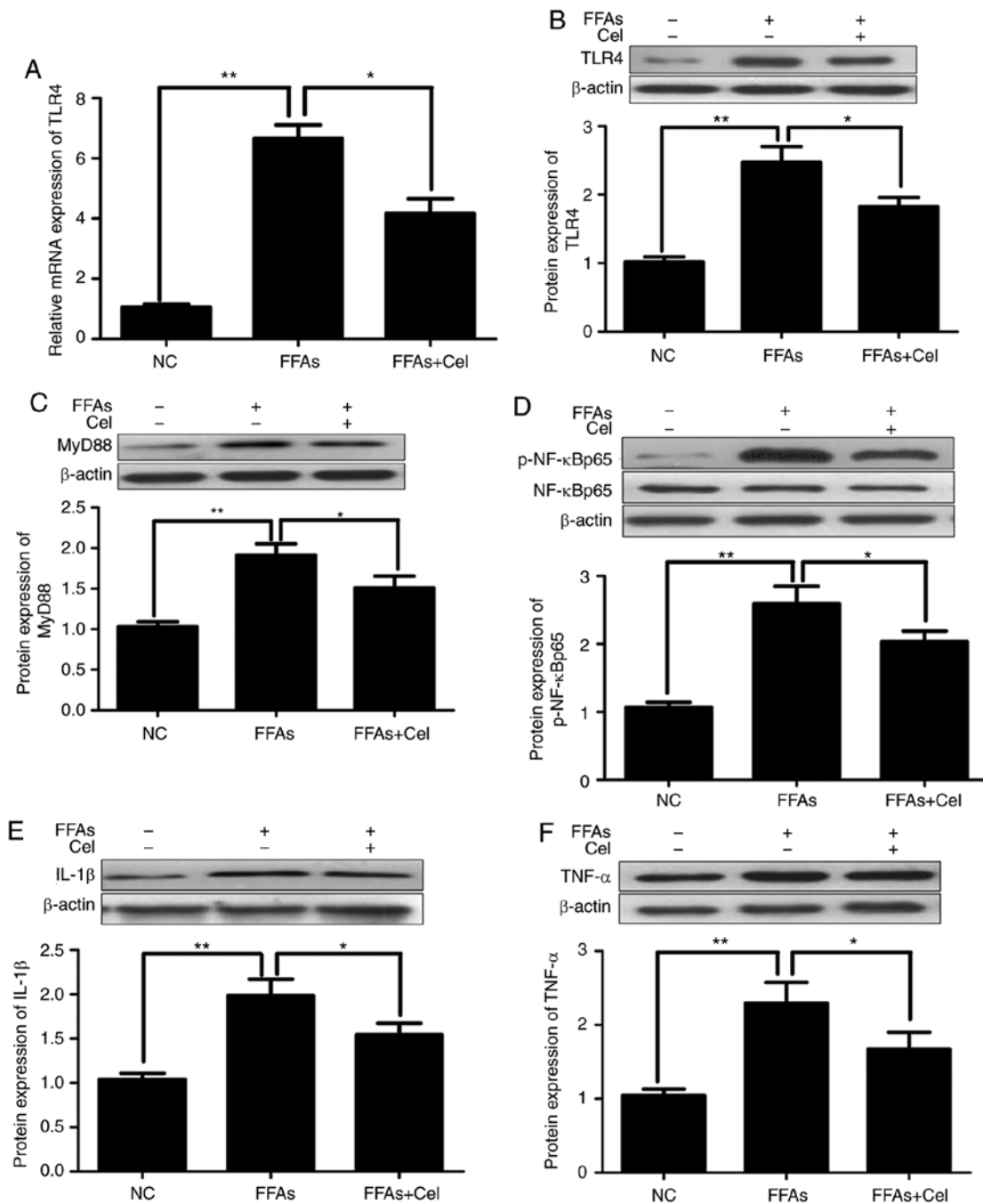


Figure 3. Celastrol administration downregulated TLR4 and downstream signaling factors in the FFA-induced HepG2 cells. HepG2 cells were cultured with 0.5  $\mu$ M celastrol and 0.5 mM FFA for 24 h, and the transcripts and protein expression levels of inflammatory mediators were analyzed by reverse transcription-quantitative polymerase chain reaction and western blotting. (A) Relative mRNA and (B) protein expression levels of TLR4. Relative protein expression levels of (C) MyD88, (D) phospho-NF- $\kappa$ Bp65 and total NF- $\kappa$ Bp65 (p-NF- $\kappa$ Bp65 levels were normalized to total NF- $\kappa$ Bp65 levels), (E) IL-1 $\beta$ , and (F) TNF $\alpha$  were assayed by western blotting. Data are expressed as the mean  $\pm$  standard error of the mean (n=6). \*P<0.05 and \*\*P<0.01. FFA, free fatty acid; TLR4, toll-like receptor 4; MyD88, myeloid differentiation primary response 88; NF- $\kappa$ B, nuclear factor- $\kappa$ B; IL-1 $\beta$ , interleukin 1 $\beta$ ; TNF $\alpha$ , tumor necrosis factor  $\alpha$ .

transcripts and protein expression levels. Similar to TLR4, the protein expression levels of downstream inflammatory mediators MyD88 (Fig. 3C), p-NF- $\kappa$ Bp65 (Fig. 3D), IL-1 $\beta$  (Fig. 3E) and TNF $\alpha$  (Fig. 3F) were significantly increased in the FFA-induced HepG2 cells compared with those in the NC group, and were markedly decreased following celastrol co-administration.

*Effects of transfection with TLR4 siRNA in HepG2 cells.* FAM-labeled siRNA was transfected into HepG2 cells with

Lipofectamine® 2000. After 24 h of transfection, the transfection efficiency was observed using fluorescence microscopy. As shown in Fig. 4A, fluorescent particles within the cells indicated that siRNA was transfected successfully into the HepG2 cells.

In order to evaluate the contribution of TLR4 to the inflammatory activation in the FFA-induced HepG2 cells and silence the expression of disease gene, three TLR4 siRNA constructs were transiently transfected into HepG2 cells using Lipofectamine® 2000. As shown in Fig. 4B and C, transfection

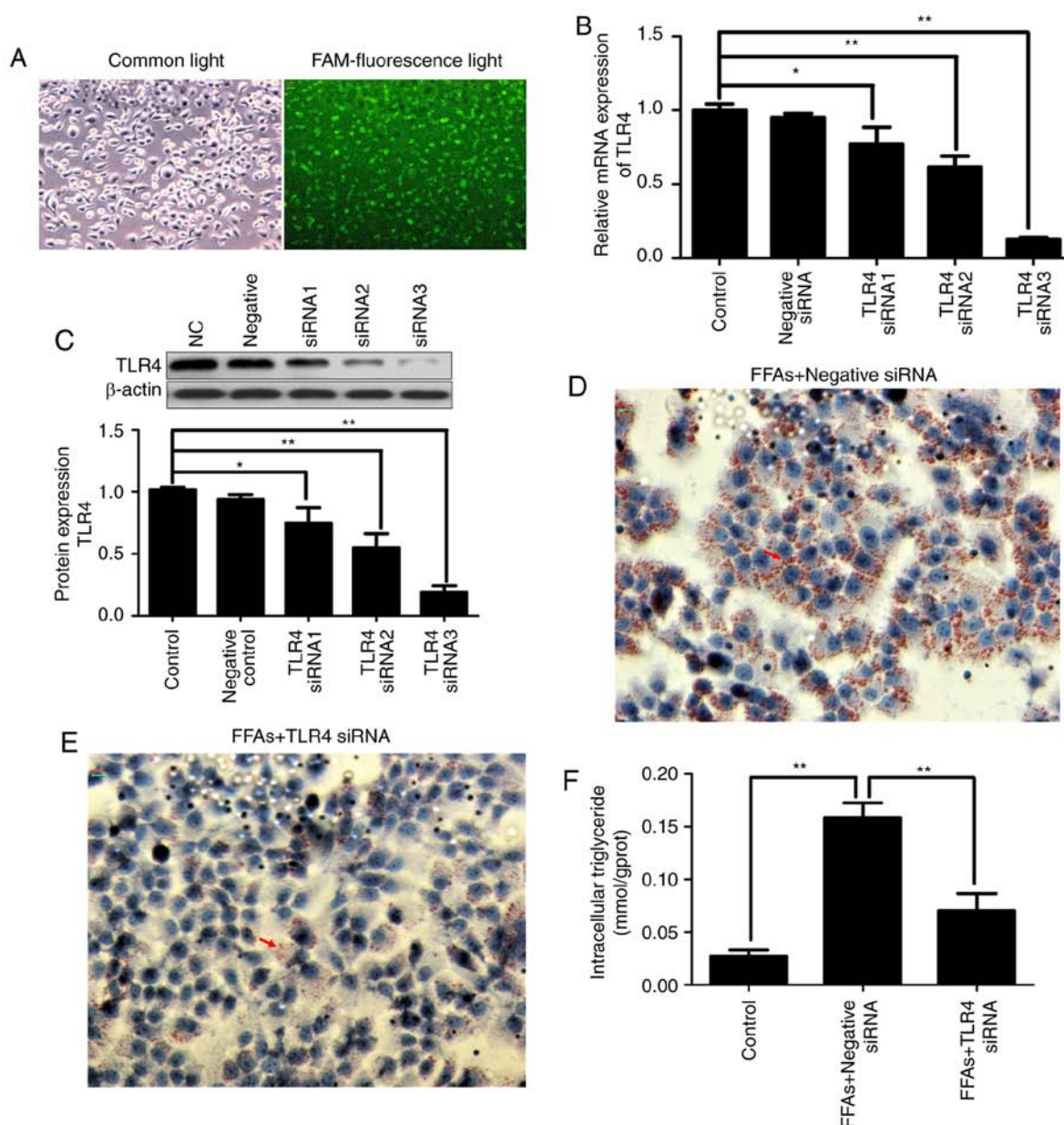


Figure 4. Effects of transfection with TLR4 siRNA in the HepG2 cells. In order to select the most effective TLR4 siRNA sequences, three FAM-labeled TLR4 siRNA constructs were transiently transfected into HepG2 cells using Lipofectamine® 2000. After 24 h of transfection, the transfection efficiency was tested by a FAM-siRNA under a fluorescence microscope (magnification, x200). (A) Visualization of the cells under common light and FAM-fluorescence light. The fluorescent particles within the cells indicated that siRNA was transfected successfully into the HepG2 cells. (B) Relative mRNA and (C) relative protein expression levels of TLR4 were analyzed by reverse transcription-quantitative polymerase chain and western blotting, respectively. (D) FFA + negative control siRNA and (E) TLR4 siRNA-treated HepG2 cells stained by Oil red O (magnification, x400). Red arrows indicate lipid droplets. (F) Levels of intracellular triglycerides were analyzed by an enzymatic assay. Data are expressed as the mean  $\pm$  standard error of the mean (n=6). \*P<0.05 and \*\*P<0.01. FFA, free fatty acid; TLR4, toll-like receptor 4; siRNA, small interfering RNA; FAM, fluorescein amidite.

with three different TLR4 siRNA constructs reduced the transcription and protein expression of TLR4 in the HepG2 cells by varying degrees. More specifically, TLR4 siRNA3 exhibited the strongest knockdown effect, inhibiting TLR4 mRNA and protein expression by ~80%. Therefore, TLR4 siRNA3 was selected for use in subsequent experiments. Notably, no effect on TLR4 expression was observed in HepG2 cells transfected with negative control siRNA.

Continuous FFA stimulation caused lipid deposition; however, when TLR4 was knocked down, FFA stimulation was also blocked. As shown in Fig. 4D and E, the increased deposition of lipid droplets in the FFA-induced HepG2 cells

was significantly decreased in the TLR4 siRNA-transfected group by Oil red O staining. As shown in Fig. 4F, the increased intracellular triglyceride content in the FFA-induced HepG2 cells was also significantly decreased in the TLR4 siRNA-transfected group.

*Celastrol protects HepG2 cells partly via the TLR4 signaling pathway.* Subsequently, experiments attempting to clarify the mechanisms underlying the modifications of FFA-induced cytokine production by celastrol were conducted. TLR4 siRNA was used to study the role of TLR4 in FFA-induced inflammation. In order to eliminate the interference of transfection

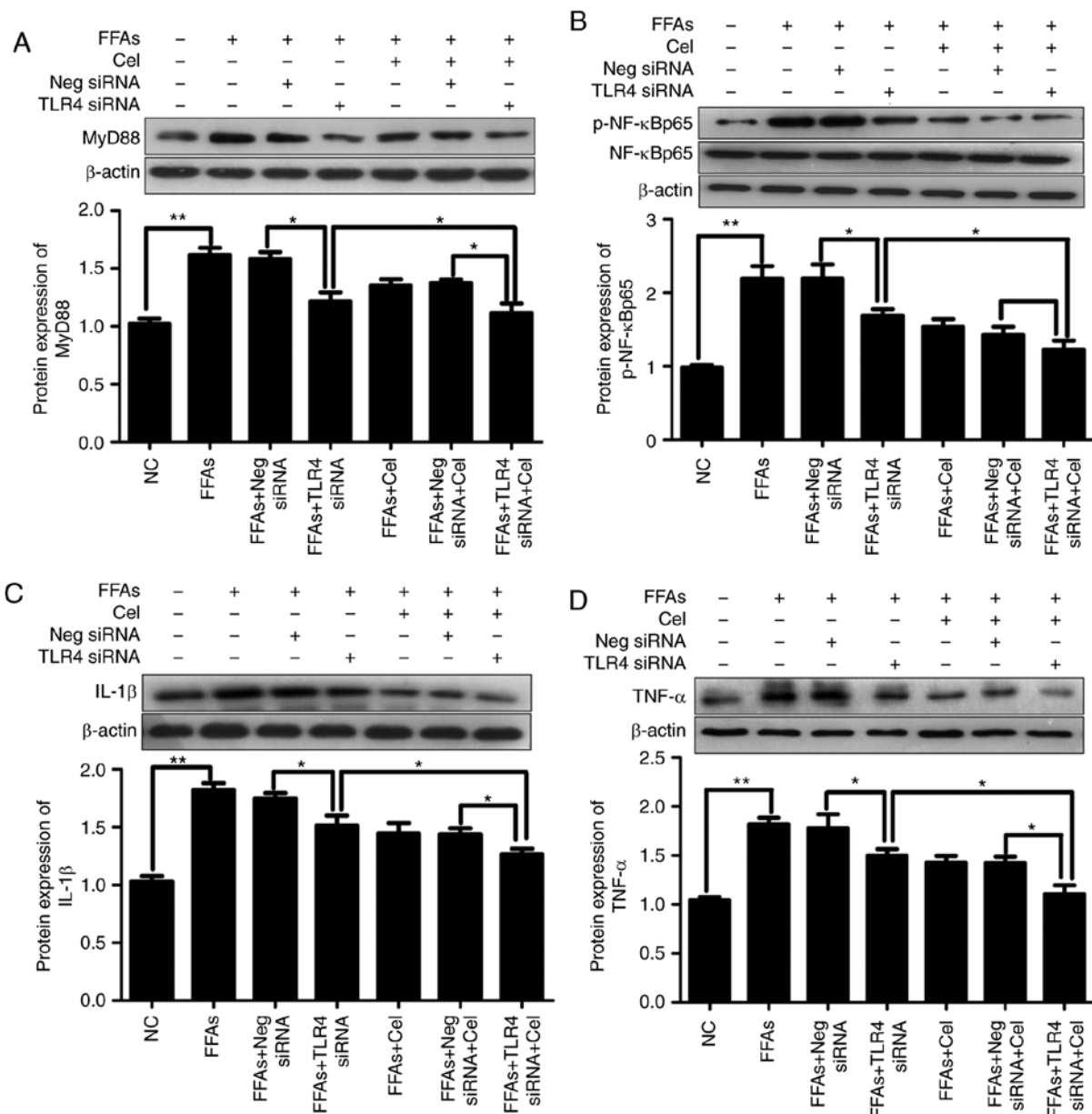


Figure 5. Effects of celastrol and TLR4 siRNA on the TLR4 signaling cascade pathway in the FFA-induced HepG2 cells. In order to understand the relative mechanisms of celastrol on ameliorating inflammatory response in the steatotic HepG2 cells, the expression levels of downstream inflammatory mediators following exposure to BSA, 0.5 mM FFA, or a mixture of FFA and 0.5  $\mu$ M celastrol for 24 h in HepG2 cells transfected with negative control siRNA or TLR4 siRNA were investigated. Relative protein expression levels of (A) MyD88, (B) phospho-NF- $\kappa$ Bp65 and total NF- $\kappa$ Bp65 (p-NF- $\kappa$ Bp65 was normalized to total NF- $\kappa$ Bp65 level), (C) IL-1 $\beta$  and (D) TNF $\alpha$  were analyzed by western blotting. Data are expressed as the mean  $\pm$  standard error of the mean (n=6). \*P<0.05 and \*\*P<0.01. FFA, free fatty acid; TLR4, toll-like receptor 4; siRNA, small interfering RNA; MyD88, myeloid differentiation primary response 88; NF- $\kappa$ B, nuclear factor- $\kappa$ B; IL-1 $\beta$ , interleukin 1 $\beta$ ; TNF $\alpha$ , tumor necrosis factor  $\alpha$ .

reagents, negative siRNA was established as a control. Thus, the expression levels of downstream inflammatory mediators were investigated subsequent to exposure to BSA, 0.5 mM FFA, or a mixture of 0.5 mM FFA and 0.5  $\mu$ M celastrol for 24 h in HepG2 cells transfected with negative control siRNA or TLR4 siRNA. As shown in Fig. 5, significantly increased activation of MyD88 (Fig. 5A), p-NF- $\kappa$ Bp65 (Fig. 5B), IL-1 $\beta$  (Fig. 5C) and TNF $\alpha$  (Fig. 5D) was observed in HepG2 cells following treatment with 0.5 mM FFA. This effect was partly dependent on TLR4, since knockdown of TLR4 alleviated the action of FFA in activating these downstream inflammatory mediators. Celastrol treatment also resulted in the inhibition of FFA-induced inflammatory response. Furthermore, celas-

trol and TLR4 siRNA co-treatment demonstrated enhanced suppressive effects as compared with each treatment alone.

## Discussion

In a previous study by our group, it was demonstrated that administration of celastrol exhibited significant suppressive effects on the levels of triglycerides, total cholesterol of hepatic tissue, and reduced steatohepatitis and macrophage infiltration in type 2 diabetic rats (15). Similar results were also observed in the present study *in vitro*. The lipid deposition and intracellular triglyceride contents were significantly higher in the FFA-induced HepG2 cells compared with those of the NC

group and markedly decreased in the celastrol-treated groups, with a higher dose of celastrol exhibiting increased efficacy.

The activation of immune and inflammatory signaling pathways is considered to be of central importance in the pathogenesis of NAFLD/NASH (22,23). Accumulating evidence in rodents and in hepatocyte cultures suggested that altered TLR4 signaling is a key pathway factor, and has an important regulatory role in stimulating the immune and inflammatory response-associated gene expression in the pathogenesis of NAFLD, and has been implicated in the progression to NASH (24,25). Xu *et al* (26) previously reported increased hepatic expression of TLR4 mRNA in rats fed with a high-fat diet compared with their control counterparts. The increase in hepatic TLR4 mRNA was associated with the appearance of NASH in this rat model (26). Furthermore, when fed with a methionine/choline-deficient diet, the most widely accepted experimental model of NASH, TLR4-deficient mice exhibited less severe hepatic injury and reduced accumulation of intrahepatic lipids compared with wild-type mice (27). The study by Sharifnia *et al* (28) also provided evidence that TLR4 was upregulated in a large cohort of NASH patients compared with those suffering from NAFLD. All these findings indicated that activation of the TLR4 signaling pathway was critically involved in the pathogenesis of NASH. The accumulation of FFA causes the activation of TLR4 signaling (29). Consistent with previous findings, the current study observed that the expression levels of TLR4 mRNA and protein were significantly increased in the FFA-induced HepG2 cells compared with those in the NC cells.

TLR4 signaling is initiated through two different pathways, the MyD88-dependent and the MyD88-independent pathways, and the latter is mediated by toll/IL-1 receptor domain-containing adaptor inducing interferon- $\beta$  (6). MyD88 is a critical downstream signaling ligand of the TLR4 receptor complex, while it is also an important adapter protein of the NF- $\kappa$ B signaling pathway, which contributes to the expression of inflammatory genes. The triggering of MyD88 pathway ultimately leads to nuclear translocation of NF- $\kappa$ Bp65 and the activation of inflammatory cascades that produce various proinflammatory cytokines, including TNF $\alpha$  and IL-1 $\beta$  (30). The study of Sharifnia *et al* (28) in a human hepatocyte culture model suggested that NF- $\kappa$ B activation was at least partially driven by hepatocyte-mediated TLR4 signaling in response to LPS and palmitate acid, with similar results observed in high-fat diet mice (31). In the present study, along with the upregulation of TLR4, the expression levels of its downstream mediators MyD88 and p-NF- $\kappa$ Bp65, as well as the cytokines IL-1 $\beta$  and TNF $\alpha$ , were consistently upregulated by FFA induction.

In order to directly determine whether TLR4 mediated the increased activities of downstream inflammatory factors upon FFA exposure, the effect of lossing the function of TLR4 was examined in HepG2 cells. TLR4 siRNA was transfected into HepG2 cells, and RT-qPCR and western blotting revealed ~80% effective TLR4 knockdown. Negative control siRNA did not affect the expression of TLR4, which indicated that the transfection effect of TLR4 siRNA was achieved through TLR4 gene inhibition, but not the transfection reagent. Next, the present study sought to determine whether TLR4 transcription was responsible for the activation of downstream inflammatory factor, as suggested by the silencing inhibition study.

Continuous FFA stimulation in the present study activated the TLR4 signaling pathways and caused lipid deposition; however, when TLR4 was knocked down, FFA stimulation was also blocked. The increased deposition of lipid droplets and intracellular triglyceride content in the FFA-induced HepG2 cells were significantly decreased in the TLR4 siRNA-transfected groups. As a consequence of limited TLR4 involvement, downstream mediators MyD88, p-NF- $\kappa$ Bp65, IL-1 $\beta$  and TNF $\alpha$  also exhibited partial attenuation. Taken together, these results confirmed our earlier findings that the activation of inflammatory factors in a lipotoxic environment was partially mediated through TLR4 signaling. Thus, targeting TLR4 may provide a promising intervention strategy for the prevention or treatment of NAFLD.

Similar to the siRNA effect, the data of the present study demonstrated that celastrol treatment markedly abolished the FFA-induced TLR4-mediated signaling cascade pathways. In addition, the results found that co-treatment with TLR4 siRNA and celastrol further attenuated the expression levels of downstream mediators compared with each treatment alone. These results suggested that celastrol may ameliorate the hepatic inflammation through other pathways in addition to TLR4. Previous studies have demonstrated that upregulation and activation of several other TLR family members were also involved in the innate immune response and the formation of inflammation (4,5). In total, 12 of the 13 members of the TLR family, with the exception of TLR3, associate with the common adaptor molecule MyD88 through interaction of their intracellular toll/IL-1 receptor domains to trigger inflammatory responses. Studies in animal models, as well as in human NAFLD patients, have indicated the likelihood for TLR2, TLR5, TLR6 and TLR9 to participate in the onset or progression of NAFLD (4,32,33).

A limitation of the present study is that only a preliminary experimental approach was used. Whether other TLR family members directly inhibit hepatic inflammation requires further investigation. Furthermore, the liver is an important natural immune organ composed of a diverse array of cell types, while it is also enriched in various immune cells, the majority of which have the potential to be involved in inflammation. It is clear that there are complex immune and inflammatory pathways that result in the progression of NASH, involving signaling in various cell types that are stimulated by pathogen- or damage-associated molecular patterns, as well as interaction between different cells (4,6). Thus, further research is required in Kupffer cells, and our future studies will address the effect and mechanisms of celastrol on the inflammatory response, which should provide valuable insights into the development in NAFLD.

In conclusion, the TLR4-mediated signaling cascade pathway may be a useful novel therapeutic target in the progression of NAFLD. The present study provided evidence that celastrol exerted its protective effects through improved triglyceride accumulation, as well as inhibition of pro-inflammatory processes. Elucidating the underlying mechanisms by which celastrol modulates hepatic steatosis may provide the molecular basis for developing therapeutic agents against NAFLD.

## Acknowledgements

Not applicable.



## Funding

The present study was supported by the National Natural Science Foundation of China (grant no. 81470187).

## Availability of data and materials

All data generated or analyzed during this study are included in this published article.

## Authors' contributions

LC conceived and designed the experiments. CL and YX performed the data analysis. LH conducted all experiments and wrote the manuscript. BS revised the manuscript. All authors read and approved the final manuscript.

## Ethics approval and consent to participate

Not applicable.

## Patient consent for publication

Not applicable.

## Competing interests

The authors declare that they have no competing interests.

## References

- Arrese M, Cabrera D, Kalergis AM and Feldstein AE: Innate immunity and inflammation in NAFLD/NASH. *Dig Dis Sci* 61: 1294-1303, 2016.
- Tiniakos DG, Vos MB and Brunt EM: Nonalcoholic fatty liver disease: Pathology and pathogenesis. *Annu Rev Pathol* 5: 145-171, 2010.
- Huang S, Rutkowski JM, Snodgrass RG, Ono-Moore KD, Schneider DA, Newman JW, Adams SH and Hwang DH: Saturated fatty acids activate TLR-mediated proinflammatory signaling pathways. *J Lipid Res* 53: 2002-2013, 2012.
- Ganz M and Szabo G: Immune and inflammatory pathways in NASH. *Hepatology* 7 (Suppl 2): S771-S781, 2013.
- Petrasek J, Csak T and Szabo G: Toll-like receptors in liver disease. *Adv Clin Chem* 59: 155-201, 2013.
- Bieghs V and Trautwein C: Innate immune signaling and gut-liver interactions in non-alcoholic fatty liver disease. *Hepatobiliary Surg Nutr* 3: 377-385, 2014.
- Kizilias S: Toll-like receptors in pathophysiology of liver diseases. *World J Hepatol* 8: 1354-1369, 2016.
- Farrell GC, van Rooyen D, Gan L and Chitturi S: NASH is an inflammatory disorder: Pathogenic, prognostic and therapeutic implications. *Gut Liver* 6: 149-171, 2012.
- Wang Y, Tu Q, Yan W, Xiao D, Zeng Z, Ouyang Y, Huang L, Cai J, Zeng X, Chen YJ and Liu A: CXCL19 suppresses proliferation and inflammatory response in LPS-induced human hepatocellular carcinoma cells via regulating TLR4-MyD88-TAK1-mediated NF- $\kappa$ B and MAPK pathway. *Biochem Biophys Res Commun* 456: 373-379, 2015.
- Venkatesha SH, Astry B, Nanjundiah SM, Yu H and Moudgil KD: Suppression of autoimmune arthritis by Celastrol through modulation of pro-inflammatory chemokines. *Bioorg Med Chem* 20: 5229-5234, 2012.
- Wang Y, Cao L, Xu LM, Cao FF, Peng B, Zhang X, Shen YF, Uzan G and Zhang DH: Celastrol ameliorates EAE induction by suppressing pathogenic T cell responses in the peripheral and central nervous systems. *J Neuroimmune Pharmacol* 10: 506-516, 2015.
- Liu J, Lee J, Salazar Hernandez MA, Mazitschek R and Ozcan U: Treatment of obesity with celastrol. *Cell* 161: 999-1011, 2015.
- Zhu F, Li C, Jin XP, Weng SX, Fan LL, Zheng Z, Li WL, Wang F, Wang WF, Hu XF, *et al*: Celastrol may have an anti-atherosclerosis effect in rabbit experimental carotid atherosclerosis model. *Int J Clin Exp Med* 7: 1684-1691, 2014.
- Kim JE, Lee MH, Nam DH, Song HK, Kang YS, Lee JE, Kim HW, Cha JJ, Hyun YY, Han SY, *et al*: Celastrol, an NF- $\kappa$ B inhibitor, improves insulin resistance and attenuates renal injury in db/db mice. *PLoS One* 8: e62068, 2013.
- Han LP, Li CJ, Sun B, Xie Y, Guan Y, Ma ZJ and Chen LM: Protective effects of celastrol on diabetic liver injury via TLR4/MyD88/NF- $\kappa$ B signaling pathway in type 2 diabetic rats. *J Diabetes Res* 2016: 2641248, 2016.
- López-Terrada D, Cheung SW, Finegold MJ and Knowles BB: HepG2 is a hepatoblastoma-derived cell line. *Hum Pathol* 40: 1512-1515, 2009.
- Gómez-Lechón MJ, Donato MT, Martínez-Romero A, Jiménez N, Castell JV and O'Connor JE: A human hepatocellular in vitro model to investigate steatosis. *Chem Biol Interact* 165: 106-116, 2007.
- Xu F, Li Z, Zheng X, Liu H, Liang H, Xu H, Chen Z, Zeng K and Weng J: SIRT1 mediates the effect of GLP-1 receptor agonist exenatide on ameliorating hepatic steatosis. *Diabetes* 63: 3637-3646, 2014.
- Cheng S, Liang S, Liu Q, Deng Z, Zhang Y, Du J, Zhang Y, Li S, Cheng B and Ling C: Diosgenin prevents high-fat diet-induced rat non-alcoholic fatty liver disease through the AMPK and LXR signaling pathways. *Int J Mol Med* 41: 1089-1095, 2018.
- Schwartz DM and Wolins NE: A simple and rapid method to assay triacylglycerol in cells and tissues. *J Lipid Res* 48: 2514-2520, 2007.
- Livak KJ and Schmittgen TD: Analysis of relative gene expression data using real-time quantitative PCR and the 2<sup>-</sup>(Delta Delta C(T)) method. *Methods* 25: 402-408, 2001.
- Takaki A, Kawai D and Yamamoto K: Molecular mechanisms and new treatment strategies for non-alcoholic steatohepatitis (NASH). *Int J Mol Sci* 15: 7352-7379, 2014.
- Szabo G and Petrasek J: Inflammasome activation and function in liver disease. *Nat Rev Gastroenterol Hepatol* 12: 387-400, 2015.
- Kesar V and Odin JA: Toll-like receptors and liver disease. *Liver Int* 34: 184-196, 2014.
- Bieghs V and Trautwein C: The innate immune response during liver inflammation and metabolic disease. *Trends Immunol* 34: 446-452, 2013.
- Xu ZJ, Fan JG, Wang XP and Wang GL: Upregulating expressions of hepatic lipopolysaccharide receptors in nonalcoholic steatohepatitis rats. *Zhonghua Gan Zang Bing Za Zhi* 14: 49-52, 2006 (In Chinese).
- Rivera CA, Adegboyega P, van Rooijen N, Tagalicud A, Allman M and Wallace M: Toll-like receptor-4 signaling and Kupffer cells play pivotal roles in the pathogenesis of non-alcoholic steatohepatitis. *J Hepatol* 47: 571-579, 2007.
- Sharifnia T, Antoun J, Verriere TG, Suarez G, Wattacheril J, Wilson KT, Peek RM Jr, Abumrad NN and Flynn CR: Hepatic TLR4 signaling in obese NAFLD. *Am J Physiol Gastrointest Liver Physiol* 309: G270-G278, 2015.
- Shen YF, Zhang X, Wang Y, Cao FF, Uzan G, Peng B and Zhang DH: Celastrol targets IRAKs to block Toll-like receptor 4-mediated nuclear factor- $\kappa$ B activation. *J Integr Med* 14: 203-208, 2016.
- Mehal WZ: The inflammasome in liver injury and non-alcoholic fatty liver disease. *Dig Dis* 32: 507-515, 2014.
- Wang N, Wang H, Yao H, Wei Q, Mao XM, Jiang T, Xiang J and Dila N: Expression and activity of the TLR4/NF- $\kappa$ B signaling pathway in mouse intestine following administration of a short-term high-fat diet. *Exp Ther Med* 6: 635-640, 2013.
- Arias-Loste MT, Iruizubieta P, Puente A, Ramos D, Santa Cruz C, Estébanez A, Llerena S, Alonso-Martín C, San Segundo D, Álvarez L, *et al*: Increased expression profile and functionality of TLR6 in peripheral blood mononuclear cells and hepatocytes of morbidly obese patients with non-alcoholic fatty liver disease. *Int J Mol Sci* 17: E1878, 2016.
- Miura K and Ohnishi H: Role of gut microbiota and Toll-like receptors in nonalcoholic fatty liver disease. *World J Gastroenterol* 20: 7381-7391, 2014.



This work is licensed under a Creative Commons Attribution-NonCommercial-NoDerivatives 4.0 International (CC BY-NC-ND 4.0) License.